Single-unit and 2-deoxyglucose studies of side inhibition in macaque striate cortex

(visual cortex/side stopping/side-band inhibition/surround inhibition/contour perception)

RICHARD T. BORN* AND ROGER B. H. TOOTELL

Department of Neurobiology, Harvard Medical School, 220 Longwood Avenue, Boston, MA 02115

ABSTRACT In the course of studies to map spatial frequency tuning of neurons in layers 2 and 3 of macaque striate cortex, we found that a high proportion (70%) of cells in the interblob regions responded poorly to full-field gratings, compared with responses to single bars, edges, or delimited gratings. This was most often due to side inhibition, in which increasing the number of cycles of a grating placed within the cell's receptive field causes progressive inhibition of response. Quantitative receptive-field mappings showed, however, that the inhibition can occur within the region activated by a bar, as well as beyond it. The inhibition appears to be orientation-selective, in that a surround grating was more effective at inhibiting the response to a center grating patch if it was of similar orientation. 2-Deoxyglucose experiments confirmed that side inhibition is very widespread in the interblobs of layers 2 and 3 and suggested that it is reduced or lacking in layers 4A through 6. Since layers 2 and 3 of striate cortex are the major source of cortical projections to area V2 and beyond, the prevalence of side stopping in these laminae has implications for theories of cortical visual function. Side-stopped interblob cells may be acting as "contour-pass filters" that filter out redundant information in textured or noisy surfaces, focusing subsequent form processing on contrasts corresponding to object boundaries.

This study was initiated as a direct result of our efforts to determine spatial frequency tuning curves from single neurons in layers 2 and 3 of macaque striate cortex (1). We found that a majority of complex cells in the interblob regions gave very poor responses to spatially extended gratings, regardless of their spatial or temporal frequency. We could always obtain an excellent response from these same cells, however, if we used a single edge or bar of light. We subsequently discovered that a grating response could be obtained if we masked off the stimulus from the sides, parallel to the preferred axis of orientation.

Since the original description of inhibitory side bands in simple cells of cat striate cortex (2), many investigators have studied a similar property in various visual cortical neurons (3–10). In the cat, side inhibition appears to show both orientation (4–7, 9) and spatial frequency (4) selectivity and to extend well beyond the bar-responsive region or classical receptive field (i.e., the area over which the cell gives an excitatory response to a single bar of light) (5, 7). In the monkey, however, less is known. De Valois *et al.* (10) showed several examples of neurons in unknown layers of macaque striate cortex that gave a reduced response as more cycles of a grating were included, a property they named "side stopping." The relationship of the property to the bar-responsive region and whether or not it displayed orientation selectivity were not addressed. In area V3A of the

macaque, Gaska *et al.* (11) reported a decreased response to wider grating patches that took place completely within the bar-responsive region.

We set out to examine several issues concerning side inhibition in striate cortex of the macaque monkey: (*i*) the spatial extent of the inhibition with respect to the borders of the bar-responsive region, (*ii*) the presence or absence of orientation selectivity in the surround, (*iii*) the relation between end stopping and side inhibition, and (*iv*) the horizontal and laminar distribution of side inhibition within striate cortex. Preliminary accounts of this work have appeared (12, 13).

MATERIALS AND METHODS

Physiological recordings, stimulus generation, and histology were as described in the preceding paper (1). The 2-deoxyglucose experiments were performed on two additional monkeys by methods described previously (14).

RESULTS

We looked for the presence or absence of side inhibition in 93 single units from interblob areas in layers 2 and 3 of macaque striate cortex. Sixty-three cells were studied during the course of the spatial frequency mapping penetrations (1), and the remaining 30 cells were studied in four additional animals used in other studies.

To quantify the inhibition, we chose a sinusoidal grating of spatial and temporal frequencies that corresponded to the width and speed of a bar to which the cell responded best, when tested qualitatively. If the cell was end-stopped, we shortened the grating to an optimal length. The grating was then centered on the cell's receptive field, and responses were measured as a function of the width of the grating patch, which was increased symmetrically about the center of the receptive field. The luminance of the screen surrounding the grating patch was equal to the mean luminance of the grating. As the width of the grating patch was varied, many cells gave a response like that shown in Fig. 1A.

We compared the spatial extent of the inhibition with the region over which the cell would respond to a light bar on a dark background (or a dark bar on a light background), subsequently referred to as the bar-responsive region. This region was carefully mapped by listening to the unit's spike discharge over a loudspeaker while making small sweeps with a thin bar. The region's lateral borders were defined as the location at which a modulated response was first detectable. For the cell in Fig. 1A virtually all of the inhibition was within the bar-responsive region, but this was not always the case, as shown in Fig. 1B. Here, further inhibition was produced by increasing the grating width beyond the bar-responsive region. Fig. 2 compares the limits of the bar-responsive region

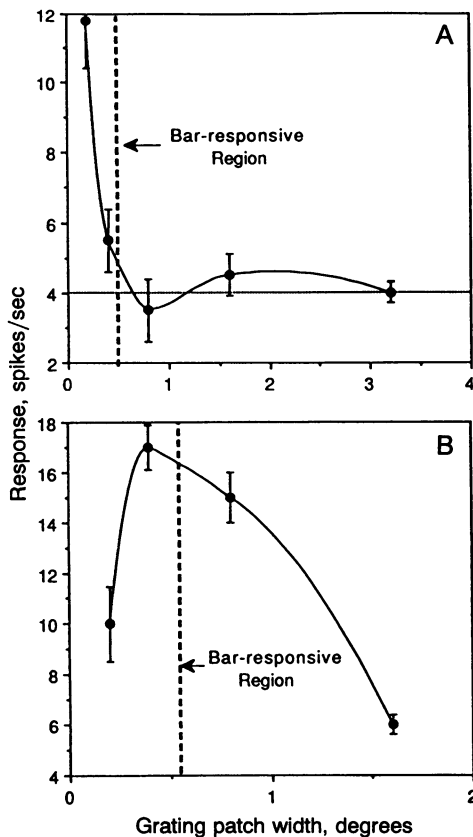*To whom reprint requests should be addressed.

FIG. 1. Side inhibition in two complex cells from macaque supragranular striate cortex. (A) Inhibition completely within the bar-responsive region. The unit was stimulated with a 7.0-cycle/degree sinusoidal grating patch of various widths. Spatial and temporal frequencies of the stimulus were held constant in all trials. The dashed vertical line indicates the region of the visual field over which the cell could be activated by a light bar on a dark background (0.6 degree wide). The horizontal line represents the level of spontaneous activity. (B) Inhibition beyond the bar-responsive region. Stimulus conditions are as in A except that the spatial frequency was 4.6 cycles/degree. The bar-responsive region for this cell was 0.53 degree wide. The cell's spontaneous activity was 1 spike/sec.

with the location of the half-inhibition point (i.e., the grating patch width at which the cell's response was reduced to half of its maximum) for 19 of the 65 side-stopped cells. While in
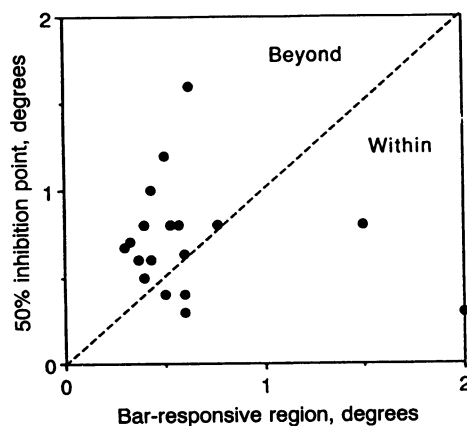

FIG. 2. Comparison of the limits of the bar-responsive region with the half-inhibition point for 19 side-stopped cells. The half-inhibition point was defined as the grating patch width at which the cell's response was reduced to half its maximum value. Points above the dashed diagonal line indicate cells whose inhibitory zones extended beyond the bar-responsive region.

some cases a significant amount of inhibition occurs within the bar-responsive region, it often extends beyond this area.

To see how many cycles of a given grating were optimal, we plotted the response of each cell against the number of cycles in the grating of a spatial frequency to which the cell gave its best response (whether delimited or extended). We then determined two parameters from each inhibition curve: the number of cycles at which the cell gave its best response and the number of cycles at which the response was half-maximal. Fig. 3 shows histograms of these two parameters for 33 side-stopped complex cells recorded in layers 2 and 3. On average, 1.3 ± 0.6 cycles of a grating gave the optimal response, and adding ≈2 more cycles reduced the firing rate by 50% (3.5 ± 1.7 cycles).

To learn whether the inhibition beyond the bar-responsive region was orientation-selective, we used a stimulus that consisted of two grating patches, a center and a surround, for which the orientation could be independently controlled. For the cell of Fig. 4, the inhibition was maximal when the surround grating was parallel to the center grating, diminished or absent when the orientation was perpendicular, and moderate at intermediate orientations. Although we have not tested surround-orientation tuning in a large enough number of cells ($n = 6$) to make conclusions about the entire population, we have seen some degree of surround-orientation selectivity in all of these side-inhibited neurons.

Prevalence and Anatomical Localization of Side Inhibition. A cell was classified as side-inhibited if its response to an extended grating was less than half of its response to a delimited grating of the same spatial frequency. By this criterion, 70% (65 of 93) of the upper-layer interblob cells were side-stopped. By way of comparison, we found end stopping in only 21% of the same population of neurons. Of the 65 cells inhibited by multiple cycles, 18 (28%) were also end-stopped. χ^2 analysis showed that the two properties behave independently ($P > 0.99$).

To gain a better appreciation of the prevalence of side inhibition and to look for the presence of topographic and laminar variations, we did two experiments using 2-deoxyglucose. The stimulus for the upper visual hemifield stimulus was a high-contrast vertical square-wave grating, with a spatial frequency of 4.5 cycles/degree, drifting to and fro (the direction was reversed every 5 sec) at a speed of 1.3 degrees/sec. In the lower hemifield, separated from the upper field by a blank strip 0.2 degree wide, a rectangular-wave grating was drifted at the same speed. The duty cycle of the rectangular grating was 0.2, and the spatial frequency was 1.8 cycles/degree. Thus, in both the rectangular and square-wave gratings, the light bars were of the same width, but the spacing
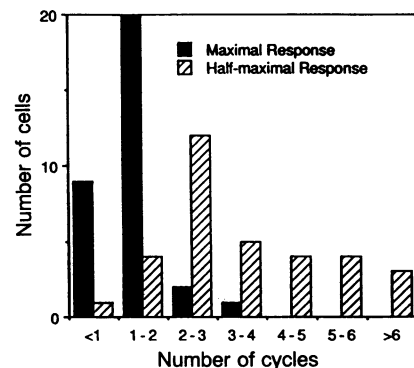

FIG. 3. Population distributions of cells showing side inhibition. Black bars, number of cycles of a sinusoidal grating to which the cell gave a maximal response; hatched bars, number of cycles of a sinusoidal grating at which the cell's response was reduced to half its maximum.

Neurobiology: Born and Tootell

Proc. Natl. Acad. Sci. USA 88 (1991) 7073

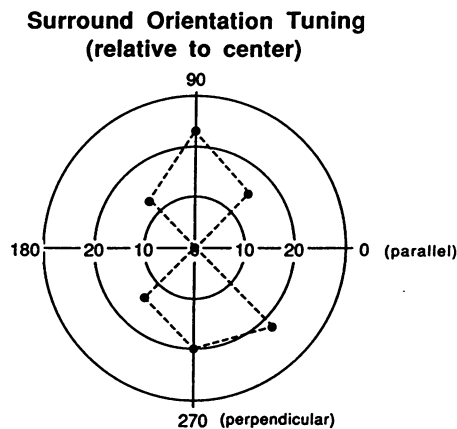**Surround Orientation Tuning
(relative to center)**

FIG. 4. Orientation dependence of multicycle inhibition. The orientation of the center grating patch was held constant while the orientation of the surround grating was varied. The center patch measured 0.37 × 0.75 degree to fill the bar-responsive region. The surround patch measured 4.0 × 4.0 degrees.

between them was 2.5 times greater in the rectangular grating.

We chose the spacing based on our single-unit data. Complex cells at an eccentricity of 4–6 degrees have receptive field widths of ≈0.5 degree. The high-frequency grating thus placed slightly over 2 cycles in the average cell's receptive field at any given time, whereas the rectangular grating would appear as a single bar at a time. Since both gratings were drifted at the same speed, cells with receptive fields in the lower visual hemifield were stimulated with 60% fewer bars. But if a significant proportion of the cells in an area were side-stopped and responded well to single bars and very poorly to high-frequency gratings, then the rectangular-wave grating might produce greater isotope uptake.

An anesthetized, paralyzed macaque was injected with 2-deoxy[^{14}C]glucose (50 μCi/kg of body weight; 1 μCi = 37 kBq) while it viewed the stimulus monocularly. Forty-five minutes later the animal was deeply anesthetized with sodium pentobarbital and perfused transcardially with fixative. The tissue was processed (1) and sections were apposed to x-ray film for 6 weeks.

The results are shown in Fig. 5. In the upper layers, at

eccentricities of 3–7 degrees, the rectangular-wave grating clearly produced greater uptake than the square-wave grating, as would be predicted if most cells are inhibited by multiple grating cycles. Comparison of the 2-deoxyglucose patterns with the cytochrome oxidase activity showed the isotope uptake to be predominantly in the interblob regions (data not shown). The dramatic difference in overall uptake within the upper layers thus supports and extends our physiological data, indicating that side stopping is an important characteristic of interblob cells in layers 2 and 3 of striate cortex.

For comparison, a section is shown including the geniculostriate input layer of the parvocellular system, 4Cβ, which can be seen as the two regions of dark/light ocular dominance stripes on either side of the retinotopic strip. Layer 4Cβ shows a reversal of the pattern of uptake in layers 2 and 3—greater uptake produced by the high-frequency grating than by the rectangular-wave grating—as one would expect for cells that are not side-inhibited. Only in the supragranular layers did the rectangular-wave grating produce greater uptake than the square-wave grating. This supports our electrophysiological impression that side inhibition is present predominantly in layers 2 and 3.

We have confirmed this basic result in one other animal with two modifications. First, a sinusoidal grating of the same spatial frequency replaced the high-spatial-frequency square-wave grating in the upper visual hemifield. This was done to show that it was not the sharp edges of the square waves that made the previous stimulus a poor one. Second, the stimulus in this case was viewed binocularly. The eyes were converged using a Risley prism to align each eye's receptive field while recording from a binocular single unit. The results in striate cortex were identical to those of Fig. 5, except for the expected lack of ocular dominance columns.

Thus, the 2-deoxyglucose results appear to reflect the presence of side inhibition in supragranular striate cortex. An alternative explanation, however, is that it was the lower spatial frequencies present in the power spectrum of the rectangular-wave grating that produced greater isotope uptake. Two considerations suggest this is not so. (*i*) Our physiological data showed that the only cells that respond preferentially to low spatial frequencies in the upper layers of striate cortex are the blob cells (1), and the blobs were only weakly labeled in the above experiment. (*ii*) The stimulus was

LAYER: 2/3 4Cв

STIMULUS:

RECTANGULAR WAVE
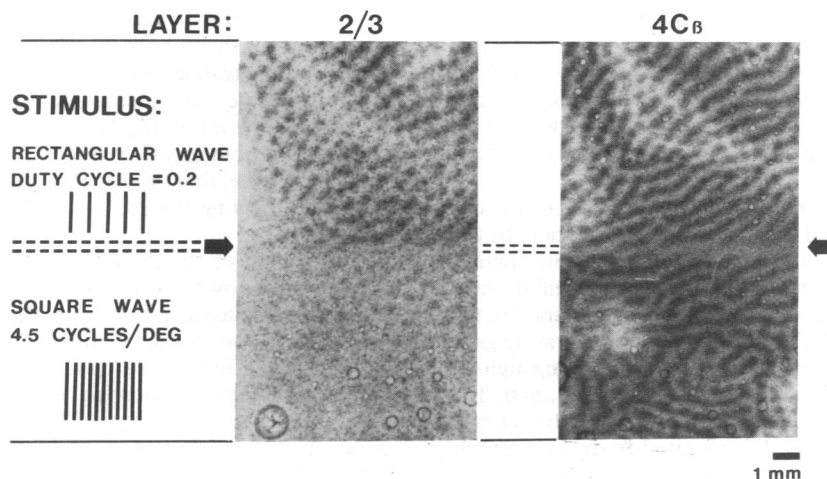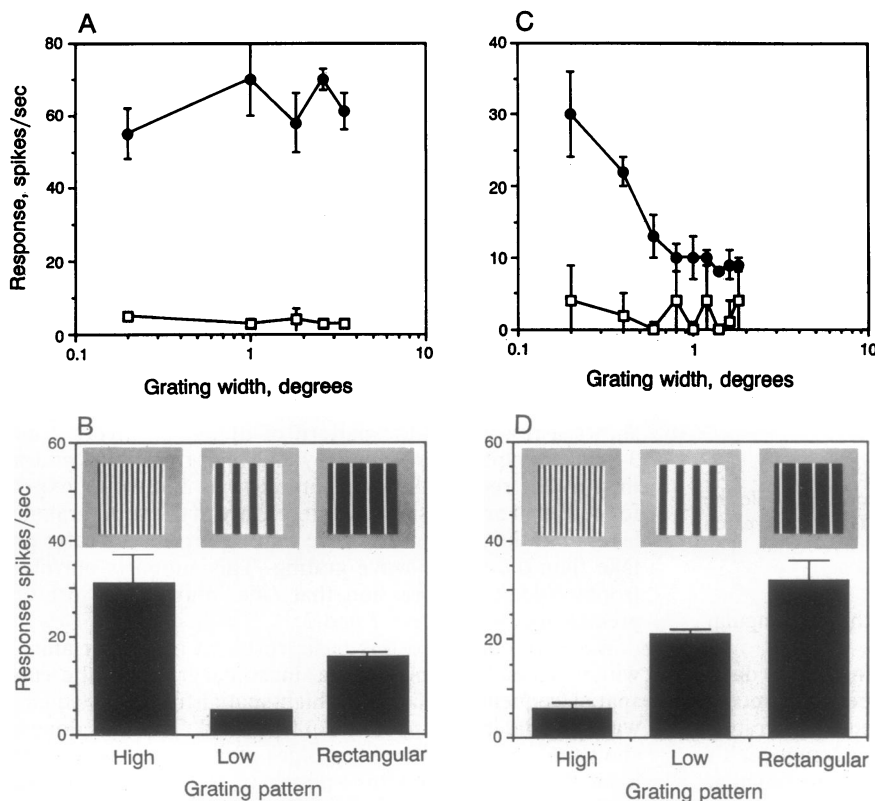DUTY CYCLE = 0.2

SQUARE WAVE
4.5 CYCLES/DEG

1 mm

FIG. 5. Results of a 2-deoxyglucose experiment in which the animal monocularly viewed the following stimulus: in the upper visual hemifield (lower half of diagram), a 4.5-cycle/degree square-wave grating; in the lower hemifield (upper half of diagram), a rectangular-wave grating containing bars of the same width as the square-wave grating but with cycles eliminated to make a duty cycle of 0.2. Both stimuli were drifted at the same speed of 1.3 degrees/sec and were of identical contrast. They were separated by a black strip 0.2 degree wide running along the horizontal meridian. In the upper layers (2/3) the rectangular wave produced greater uptake despite the fact that any given cell saw fewer bars per unit time compared with the square-wave grating. In the geniculate parvocellular input layer, the situation was reversed, with greater uptake produced by the square-wave grating. Note: the stimulus diagrams in this figure are the opposite contrast of those viewed by the animal.

FIG. 6. Responses of single units to a rectangular wave and its high- and low-spatial-frequency components. A and B show data from a non-side-stopped unit. C and D are from a different, side-stopped unit. (A) Side inhibition curve at a spatial frequency of 8.4 cycles/degree. The cell shows no inhibition. ●, Response to the stimulus; □, response to a blank field of the same mean luminance as the gratings. (B) Response of the same cell to the stimuli depicted above each data point. High, 8.4-cycle/degree sinusoidal grating; low, 4.2-cycle/degree sinusoidal grating; rectangular, duty cycle of 0.2 at a frequency of 4.2 cycles/degree. (C) Side-inhibition curve obtained with a sinusoidal grating of 4.6 cycles/degree. ●, Response to the stimulus; □, spontaneous activity prior to each trial. (D) Response of the same cell to the stimuli depicted above each data point. High, 4.6-cycle/degree sinusoidal grating; low, 2.3-cycle/degree sinusoidal grating; rectangular, duty cycle of 0.25 at a frequency of 2.3 cycles/degree. The patch size was 2.0 × 2.0 degrees.

achromatic, and single-orientation achromatic stimuli activate blob cells poorly in 2-deoxyglucose studies (ref. 15; R.B.H.T., unpublished data).

We nevertheless wanted to test this possibility with single-unit physiology. Therefore we essentially repeated the 2-deoxyglucose experiment on single interblob cells that were either side-stopped or not. We first determined a curve for side inhibition, as previously described, and then presented the cell with three additional full-field stimuli in a randomly interleaved manner: (i) a high-spatial-frequency sinusoidal grating, (ii) a rectangular-wave grating in which the white bars were the width of one-half cycle of the high-frequency grating but more widely spaced, corresponding to a duty cycle of 0.25 or 0.20, and (iii) a low-spatial-frequency sinusoidal grating that corresponded to the spacing of the bars in the rectangular-wave grating. We reasoned that if the 2-deoxyglucose result were due to a preference for low spatial frequencies, the low-spatial-frequency sinusoidal grating should actually be a better stimulus than the rectangular wave since it would not be contaminated with high spatial frequencies.

Typical results are shown in Fig. 6. For a cell that was not side-stopped (Fig. 6 A and B), the response was best to the high-spatial-frequency grating, worst to the low-spatial-frequency grating, and intermediate to the rectangular-wave grating (Fig. 6B). For a side-stopped unit (Fig. 6 C and D), the result was quite different. The rectangular-wave grating gave a much better response than either the corresponding high- or low-spatial-frequency sinusoidal components (Fig. 6D). The width of this cell's receptive field measured with a bar of light was 0.43 degree; thus for the high-spatial-frequency grating there were always 2 full cycles in the cell's receptive field, as opposed to only 1 cycle at a time for the other two stimuli.

DISCUSSION

Our findings are in agreement with previous reports of orientation-selective suppressive surrounds in complex neurons (2–11). Two additional reports on surround effects in

striate cortex of the cat (16) and awake, behaving monkey (17) have appeared. Still other studies have noted poorer neuronal responses to multiple cycles of a grating patch vs. a single bar or edge (18–20). Side inhibition was not the primary focus of this last group of studies, yet they seem to have encountered the same basic phenomenon described here.

To this body of data on side inhibition we have added quantitative information on the spatial extent of the inhibition, showing, in particular, that a significant amount can occur within the bar-responsive region as well as beyond it. This situation, while the exception in striate cortex (Fig. 2), appears to be the rule in area V3A of the macaque (11). Our data also indicate that side inhibition and end stopping are two distinct types of inhibition, evidently reflecting a spatial anisotropy in the surrounds of these neurons. Finally, we have demonstrated by both single-unit physiology and 2-deoxyglucose functional labeling that side inhibition is common in the interblob regions of layers 2 and 3 in monkey striate cortex but greatly reduced or lacking in other laminae (Fig. 5). We feel that this functional organization is important for understanding the role of side inhibition in visual processing.

The source of the inhibitory surround for these neurons remains unknown. A possible anatomic basis for effects beyond the classical receptive field exists in the form of long-range horizontal connections of pyramidal neurons demonstrated in both cat (21, 22) and monkey (23). Cross-correlation studies showing that most of the long-range interactions are excitatory (24) are somewhat difficult to relate to the predominantly inhibitory interactions that we and others have observed. Gilbert and Wiesel (16) have attempted to reconcile these results by postulating orientation-selective facilitation (mediated by the long-range horizontal connections) of a nonoriented inhibitory surround. Preliminary data (unpublished) suggest that the source of inhibition for upper-layer side-stopped neurons may be lower-layer neurons (with larger receptive fields) that increase their firing rates as more grating cycles are added. Thus, side

inhibition may occur by a mechanism similar to that proposed for end stopping (25). A final possibility is that side stopping is produced by corticofugal inhibitory influence from larger receptive fields in higher-tier cortical areas.

Finally, we mention two classes of psychophysical observations that may be manifestations of side inhibition.

The first is "simultaneous orientation contrast" (26), in which the orientation of surround lines can alter the apparent orientation of a centrally placed test line. The possible relationship between this phenomenon and surround inhibition has been discussed recently (16) and so will not be addressed further here.

The other class of psychophysical phenomena concerns the discrimination of contours (image contrasts corresponding to object boundaries) from certain kinds of textures (multiple, parallel image contrasts corresponding to surface properties). Contour–texture discrimination has been recognized as a significant problem solved by the visual system (27) and has served as the basis for models of striate cortex (28–30) that have greatly influenced our thinking about the possible perceptual role of side inhibition.

The particular distinction we wish to draw between "contour contrasts" and "texture contrasts" is illustrated by a class of masking illusions discovered by Galli and Zama (31) and expanded by Kanizsa (32). The basic observation is that a contour is effectively hidden when flanked by additional contrasts of the same orientation. For example, the image in Fig. 7 appears to be a large square whose corners are covered by four smaller, striped squares, even though it is actually an octagon whose oblique sides have been flanked by multiple parallel lines. Without the flanking gratings, these sides would be perceived as part of the octagon (i.e., as object boundaries). Here they have been swallowed up by the striped texture, losing their status as contours. The two perceptual classifications seem to be mutually exclusive.

In these masking illusions, the "form" subsystem selectively ignores elongated image contrasts that are redundant (see ref. 33) and thus likely to belong to a surface. Side
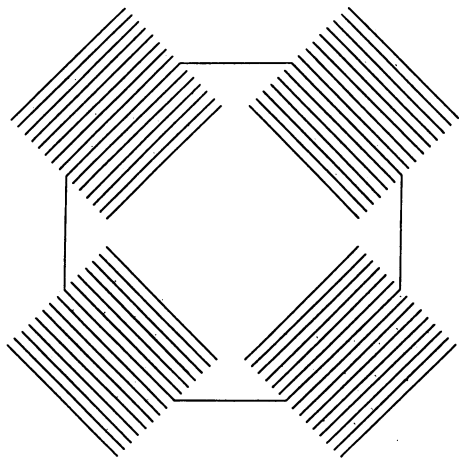

FIG. 7. Masking of contours by parallel lines (after Galli and Zama, ref. 31). The oblique sides of the octagon are swallowed up by the textured squares that overlie the four corners of the octagon. Side inhibition at different spatial scales may account for this type of illusion.

inhibition is a mechanism that could generate this property, and one might think of side-stopped cells as "contour-pass filters" that focus subsequent form processing on contrasts likely to represent object boundaries.

1. Born, R. T. & Tootell, R. B. H. (1991) *Proc. Natl. Acad. Sci. USA* **88**, 7066–7070.
2. Bishop, P. O., Coombs, J. S. & Henry, G. H. (1973) *J. Physiol. (London)* **231**, 31–60.
3. Jones, B. H. (1970) *Am. J. Physiol.* **218**, 1102–1107.
4. Blakemore, C. & Tobin, E. A. (1972) *Exp. Brain Res.* **15**, 439–440.
5. Maffei, L. & Fiorentini, A. (1976) *Vision Res.* **16**, 1131–1139.
6. Fries, W., Albus, K. & Creutzfeldt, O. D. (1977) *Vision Res.* **17**, 1001–1008.
7. Nelson, J. I. & Frost, B. J. (1978) *Brain Res.* **139**, 359–365.
8. Albus, K. & Fries, W. (1980) *Vision Res.* **20**, 369–372.
9. Ferster, D. (1981) *J. Physiol. (London)* **311**, 623–655.
10. De Valois, R. L., Thorell, L. G. & Albrecht, D. G. (1985) *J. Opt. Soc. Am.* **A2**, 1115–1123.
11. Gaska, J. P., Jacobson, L. D. & Pollen, D. A. (1987) *Vision Res.* **27**, 1687–1692.
12. Born, R. T. & Tootell, R. B. H. (1989) *Invest. Ophthalmol. Vis. Sci.* **30**, 111 (abstr.).
13. Born, R. T. & Tootell, R. B. H. (1990) *Soc. Neurosci. Abstr.* **16**, 1270.
14. Tootell, R. B. H., Hamilton, S. L., Silverman, M. S. & Switkes, E. (1988) *J. Neurosci.* **8**, 1500–1530.
15. Tootell, R. B. H., Silverman, M. S., Hamilton, S. L., Switkes, E. & De Valois, R. L. (1988) *J. Neurosci.* **8**, 1610–1624.
16. Gilbert, C. D. & Wiesel, T. N. (1990) *Vision Res.* **30**, 1689–1701.
17. Knierim, J. J. & Van Essen, D. C. (1989) *Soc. Neurosci. Abstr.* **15**, 323.
18. Schiller, P. H., Finlay, B. L. & Volman, S. F. (1976) *J. Neurophysiol.* **39**, 1334–1351.
19. Carras, P. & DeVoe, R. (1989) *Invest. Ophthal. Vis. Sci.* **30**, 69 (abstr.).
20. von der Heydt, R. & Peterhans, E. (1989) *J. Neurosci.* **9**, 1731–1748.
21. Gilbert, C. D. & Wiesel, T. N. (1983) *J. Neurosci.* **5**, 1116–1133.
22. Martin, K. A. C. & Whitteridge, D. (1984) *J. Physiol. (London)* **353**, 463–504.
23. Rockland, K. S. & Lund, J. S. (1983) *J. Comp. Neurol.* **216**, 303–318.
24. Ts'o, D. Y., Gilbert, C. D. & Wiesel, T. N. (1986) *J. Neurosci.* **6**, 1160–1170.
25. Bolz, J. & Gilbert, C. D. (1986) *Nature (London)* **320**, 362–365.
26. Westheimer, G. (1990) *Vision Res.* **30**, 1913–1921.
27. Marr, D. (1982) *Vision* (Freeman, San Francisco).
28. Grossberg, S. & Mingolla, E. (1985) *Psychol. Rev.* **92**, 173–211.
29. Grossberg, S., Mingolla, E. & Todorovic, D. (1989) *IEEE Trans. Biomed. Eng.* **36**, 65–84.
30. Blasdel, G. G. (1989) in *Sensory Processing in the Mammalian Brain*, ed. Lund, J. S. (Oxford Univ. Press, Oxford), pp. 242–267.
31. Galli, A. & Zama, A. (1931) *Z. Psychol.* **123**, 308–348.
32. Kanizsa, G. (1979) *Organization in Vision: Essays on Gestalt Perception* (Praeger, New York).
33. Attneave, F. (1954) *Psychol. Rev.* **61**, 183–193.